

Interlayer-Interaction Dependence of Latent Heat in the Heisenberg Model on a Stacked Triangular Lattice with Competing Interactions

Ryo Tamura^{1,*} and Shu Tanaka^{2,†}

¹*International Center for Young Scientists, National Institute for Materials Science,
1-2-1, Sengen, Tsukuba-shi, Ibaraki, 305-0047, Japan*

²*Department of Chemistry, University of Tokyo, 7-3-1, Hongo, Bunkyo-ku, Tokyo, 113-0033, Japan*

We study phase transition behavior of a frustrated Heisenberg model on a stacked triangular lattice by Monte Carlo simulations. The model has three types of interactions: ferromagnetic nearest-neighbor interaction J_1 and antiferromagnetic third nearest-neighbor interaction J_3 in each triangular layer and ferromagnetic interlayer interaction J_\perp . Frustration comes from the intralayer interactions J_1 and J_3 . We focus on the case that the order parameter space is $\text{SO}(3) \times C_3$. We find that the model exhibits a first-order phase transition with breaking of the $\text{SO}(3)$ and C_3 symmetries at finite temperature. We also discover that the transition temperature increases but the latent heat decreases as J_\perp/J_1 increases. This fact is opposite to behavior observed in conventional unfrustrated systems.

PACS numbers: 75.10.Hk, 64.60.De, 75.40.Mg, 75.50.Ee

I. INTRODUCTION

Geometrically frustrated systems often exhibit a characteristic phase transition, such as successive phase transitions and order by disorder, and an unconventional ground state such as spin liquid state.^{1–12} In frustrated continuous spin systems, the ground state is often non-collinear spiral spin structure. The spiral spin structure leads to exotic electronic properties such as multiferroic phenomena,^{13–17} anomalous Hall effect,¹⁸ and localization of electronic wave function.¹⁹ Then, properties of frustrated systems have been attracted attention in statistical physics and condensed matter physics. Many geometrically frustrated systems such as stacked triangular antiferromagnets (see Fig. 1), stacked kagome antiferromagnets, and spin-ice systems have been synthesized and their properties have been investigated. In theoretical studies, the relation between phase transition and order parameter space in geometrically frustrated systems has been considered.^{20–24}

As an example of phase transition nature in geometrically frustrated systems, properties of the Heisenberg model on a triangular lattice have been theoretically studied for a long time. The ground state of ferromagnetic Heisenberg model on a triangular lattice is ferromagnetically collinear spin structure. In this case, the order parameter space is S_2 . The long-range order of spins does not appear at finite temperature because of the Mermin-Wagner theorem.²⁵ The model does not exhibit any phase transitions. On the other hand, Refs. 21,26,27 reported that a topological phase transition occurs in the Heisenberg model on a triangular lattice with only antiferromagnetic nearest-neighbor interactions. In the model, the long-range order of spins is prohibited by the Mermin-Wagner theorem, and thus a phase transition driven by the long-range order of spins does not occur as well as the ferromagnetic Heisenberg model. Since the ground state of the model is the 120-degree structure,

the order parameter space is $\text{SO}(3)$ which is the global rotational symmetry of spins. Thus, the point defect, $Z_2 = \pi_1(\text{SO}(3))$ vortex defect, can exist in the model. Then, the topological phase transition occurs by dissociating the Z_2 vortices at finite temperature.^{21,26} The dissociation of Z_2 vortices is one of characteristic properties of geometrically frustrated systems when the ground state is a non-collinear spin structure in two dimension. Temperature dependence of the vector chirality and that of the number density of Z_2 vortices in the Heisenberg model on a kagome lattice were also studied.²⁸ An indication of the Z_2 vortex dissociation has been observed in electron paramagnetic resonance (EPR) and electron spin resonance (ESR) measurements.^{29–31}

Recently, another kind of characteristic phase transition nature has been found in Heisenberg models on a

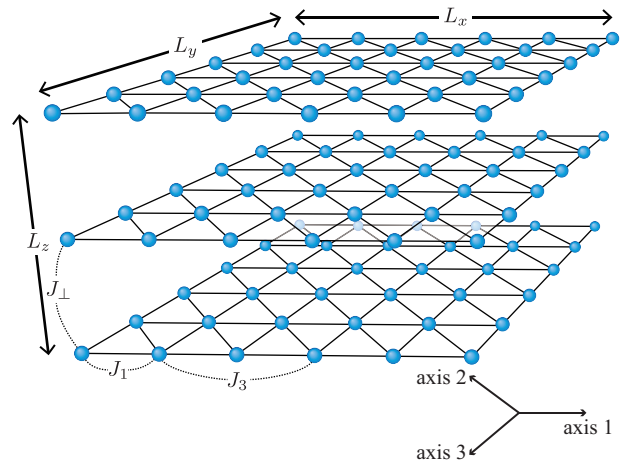


FIG. 1. (Color online) Schematic picture of stacked triangular lattice with $L_x \times L_y \times L_z$ sites. J_1 and J_3 respectively represent the nearest-neighbor and third nearest-neighbor interactions in each triangular layer and J_\perp is the interlayer interaction.

triangular lattice with further interactions.^{23,24,32,33} The order parameter space is described by the direct product between global rotational symmetry of spins $\text{SO}(3)$ and discrete lattice rotational symmetry which depends on the ground state. In these models, a phase transition with the discrete symmetry breaking occurs at finite temperature. In the J_1 - J_3 Heisenberg model on a triangular lattice, the ground state is the spiral-spin structure where C_3 lattice rotational symmetry is broken, due to the competition between ferromagnetic nearest-neighbor interaction J_1 and antiferromagnetic third nearest-neighbor interaction J_3 .^{32,33} In this case, the order parameter space is $\text{SO}(3) \times C_3$. This model exhibits a first-order phase transition with breaking of the C_3 symmetry. In addition, the dissociation of Z_2 vortices which comes from the $\text{SO}(3)$ symmetry occurs at the first-order phase transition temperature. Similar phase transition with the discrete symmetry breaking has been also found in Heisenberg models on square and hexagonal lattices with further interactions.³⁴⁻³⁷ To consider a microscopic mechanism of the first-order phase transition with the discrete symmetry breaking in frustrated continuous spin systems, a generalized Potts model, called Potts model with invisible states, has been studied.³⁸⁻⁴⁰

Phase transition in three-dimensional frustrated systems has been theoretically studied as well as that in two-dimensional frustrated systems. In many cases, phase transition nature in three-dimensional systems differs from that in two-dimensional systems. In the Heisenberg model on a stacked triangular lattice with the antiferromagnetic nearest-neighbor intralayer interaction J_1 and the nearest-neighbor interlayer interaction J_\perp , the ground state is 120-degree structure in each triangular layer. Thus, the order parameter space is $\text{SO}(3)$ as with two-dimensional case. Two types of contradictory results have been reported as follows. In one, a second-order phase transition belonging to the universality class called chiral universality class which relates to the $\text{SO}(3)$ symmetry occurs.^{3,41-45} In the other, a first-order phase transition occurs at finite temperature.⁴⁶⁻⁴⁹ In addition, phase transition in the Heisenberg model on a stacked triangular lattice with antiferromagnetic J_1 , antiferromagnetic second nearest-neighbor interaction J_2 , and J_\perp has been studied.⁵⁰⁻⁵³ In this model, many types of phase transitions depending on the ratio J_2/J_1 were reported.

The purpose of this paper is to investigate an interlayer interaction effect for phase transition behavior on the Heisenberg model on a stacked triangular lattice with competing intralayer interactions. We focus on the case that the order parameter space is described by the direct product between global spin rotational symmetry and discrete lattice rotational symmetry. We study finite-temperature properties of the J_1 - J_3 model on a stacked triangular lattice. The order parameter space of the model is $\text{SO}(3) \times C_3$ for certain parameter region whereas for other region, the order parameter space is not the direct product between two groups. As mentioned above, a first-order phase transition with the threefold symmetry

breaking occurs in the J_1 - J_3 Heisenberg model on a two-dimensional triangular lattice when the order parameter space is $\text{SO}(3) \times C_3$.^{23,32,33} We consider the interlayer interaction J_\perp dependence of phase transition nature, *e.g.*, transition temperature and latent heat.

The rest of the paper is organized as follows. In Sec. II, we introduce the J_1 - J_3 model on a stacked triangular lattice and consider the ground state of the model. The model consists of three types of interactions (see Fig. 1): ferromagnetic nearest-neighbor interaction J_1 and antiferromagnetic third nearest-neighbor interaction J_3 in each triangular layer and ferromagnetic interlayer interaction J_\perp . The intralayer interactions J_1 and J_3 cause frustration. The ground state depends on the interaction ratio J_3/J_1 regardless of J_\perp . In Sec. III, we show finite-temperature properties of the J_1 - J_3 model on a stacked triangular lattice for $J_3/J_1 = -0.85355 \dots$ and $J_\perp/J_1 = 2$ by Monte Carlo simulation. In this case, the order parameter space is $\text{SO}(3) \times C_3$. We find that the system exhibits a first-order phase transition with breaking of the C_3 lattice rotational symmetry and the $\text{SO}(3)$ symmetry of spin at finite temperature. In Sec. IV, we investigate J_\perp -dependence of phase transition behavior. We find that as J_\perp increases fixing $J_3/J_1 = -0.85355 \dots$ which is used in Sec. III, the transition temperature increases but the latent heat decreases. This fact is opposite to behavior observed in conventional unfrustrated systems. Section V is devoted to the discussion and conclusion. In Appendix A, we obtain the Curie-Weiss temperature from the magnetic susceptibility.

II. MODEL AND GROUND STATE

We study physical properties of a classical Heisenberg model on a stacked triangular lattice with the nearest-neighbor and third nearest-neighbor interactions. The Hamiltonian of the system is given by

$$\mathcal{H} = -J_1 \sum_{\langle i,j \rangle_1} \mathbf{s}_i \cdot \mathbf{s}_j - J_3 \sum_{\langle i,j \rangle_3} \mathbf{s}_i \cdot \mathbf{s}_j - J_\perp \sum_{\langle i,j \rangle_\perp} \mathbf{s}_i \cdot \mathbf{s}_j, \quad (1)$$

where \mathbf{s}_i is the three-component vector spin of unit length. The first and second sums are over all pairs of nearest-neighbor sites and that of third nearest-neighbor sites in each triangular layer (see Fig. 1). The third term represents the nearest-neighbor interlayer interactions. Here, it should be noted that the internal energy for $J_\perp > 0$ is the same as that for $-J_\perp$ by applying the local gauge transformation: $\mathbf{s}_i \rightarrow -\mathbf{s}_i$ for all spins in even numbered layers. Then, in order to consider phase transition nature, it is enough to study the case of ferromagnetic interlayer interaction ($J_\perp > 0$). Let $N = L_x \times L_y \times L_z$ be the number of spins (see Fig. 1). In this paper, we study the case that $L_x = L_y = L_z = L$.

We consider the ground state spin configuration depending on the interactions J_1 and J_3 . In general, the

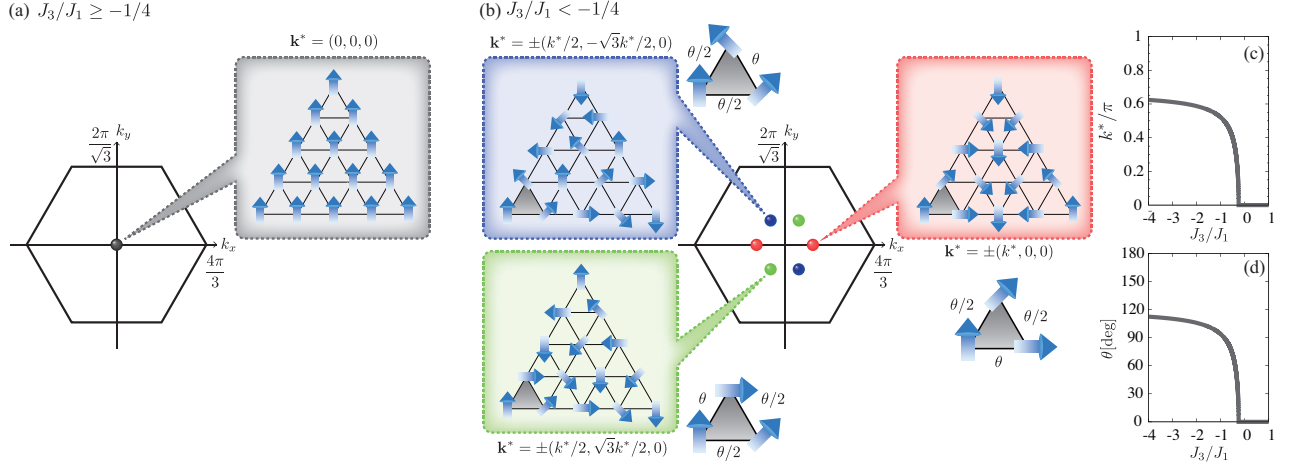


FIG. 2. (Color online) Explanation drawings of ground state properties when the nearest-neighbor interaction J_1 is ferromagnetic. (a) Position of \mathbf{k}^* which minimizes the Fourier transform of interactions and schematic of a ferromagnetic spin configuration in each triangular layer when $J_3/J_1 \geq -1/4$. (b) Position of \mathbf{k}^* and schematic of spiral-spin configurations in each triangular layer when $J_3/J_1 < -1/4$. The spin configurations are depicted for $J_3/J_1 = -0.85355 \dots$ corresponding to $k^* = \pi/2$, then $\theta = 90^\circ$. (c) J_3/J_1 -dependence of k^* . (d) J_3/J_1 -dependence of relative angle θ .

ground state of the Heisenberg model is a spiral-spin configuration^{54,55} given by

$$\mathbf{s}_i = \mathbf{R} \cos(\mathbf{k}^* \cdot \mathbf{r}_i) - \mathbf{I} \sin(\mathbf{k}^* \cdot \mathbf{r}_i), \quad (2)$$

where \mathbf{R} and \mathbf{I} are two arbitrary orthogonal unit vectors, and \mathbf{r}_i is the position vector of i -th site. The vector $\mathbf{k}^* = (k_x^*, k_y^*, k_z^*)$ minimizes the Fourier transform of interactions $J(\mathbf{k})$ given by

$$J(\mathbf{k})/N = -J_1 \cos(k_x) - 2J_1 \cos\left(\frac{1}{2}k_x\right) \cos\left(\frac{\sqrt{3}}{2}k_y\right) - J_3 \cos(2k_x) - 2J_3 \cos(k_x) \cos(\sqrt{3}k_y) - J_\perp \cos(k_z). \quad (3)$$

Here the lattice constant is set to unity. Since we now consider the case of $J_\perp > 0$, the value of k_z^* is always 0. On the other hand, when the interlayer interaction is antiferromagnetic, k_z^* is always π . Note that the spin configuration represented by \mathbf{k} is the same as that by $-\mathbf{k}$ in the Heisenberg model. \mathbf{k}^* depends on both signs of interactions and ratio of interactions J_3/J_1 .

We first consider the case that J_1 is ferromagnetic interaction ($J_1 > 0$). When $J_3/J_1 \geq -1/4$, the ground state is ferromagnetic state, *i.e.*, $\mathbf{k}^* = (0, 0, 0)$, depicted in Fig. 2(a). Then, the order parameter space is S_2 . Thus, a phase transition occurs and its universality class is expected to be the same as the three-dimensional ferromagnetic Heisenberg model. On the other hand, when $J_3/J_1 < -1/4$, the ground state is a spiral-spin structure represented by one of six wave vectors:

$$\mathbf{k}^* = \pm(k^*, 0, 0), \pm(k^*/2, \sqrt{3}k^*/2, 0), \pm(k^*/2, -\sqrt{3}k^*/2, 0), \quad (4)$$

which are depicted in Fig. 2(b). The value of $k^* = |\mathbf{k}^*|$ changes between 0 and $2\pi/3$ depending on J_3/J_1 following the relation:

$$J_3/J_1 = -\frac{1 \sin k^* + \sin \frac{1}{2}k^*}{2 \sin k^* + \sin 2k^*}. \quad (5)$$

Figure 2(c) shows J_3/J_1 -dependence of value of k^* . The relation means that the relative angle θ between nearest-neighbor spin pairs along one axis is $180k^*/\pi$ -degree, and that along the other axes is $\theta/2$. J_3/J_1 -dependence of relative angle θ is shown in Fig. 2(d). Since the system has the 120-degree lattice rotational symmetry of triangular lattice C_3 , there are three ways to be selected the axis where the relative angle between nearest-neighbor spin pairs differs from the others as represented by Eq. (4). Thus, the order parameter space for $J_3/J_1 < -1/4$ is $\text{SO}(3) \times C_3$. Next, we consider the case that J_1 is antiferromagnetic interaction ($J_1 < 0$). When $J_3/J_1 > -1/9$, the ground state is 120-degree structure *i.e.*, $k^* = 4\pi/3$ in Eq. (4). Then the order parameter space is $\text{SO}(3)$ which is the same as the order parameter space of the Heisenberg model on a stacked triangular lattice with only antiferromagnetic nearest-neighbor interaction.^{3,41-49} On the other hand, when $J_3/J_1 \leq -1/9$, there are degenerated ground states. One of the degenerated ground states is described by $\mathbf{k}^* = (0, 2\pi/\sqrt{3}, 0)$. Degenerated ground states can be generated by applying three-dimensional rotations to the spin structure represented by $\mathbf{k}^* = (0, 2\pi/\sqrt{3}, 0)$ in an appropriate way shown in Fig. 2 in Ref. 56. Then, the order parameter space is not well-defined in this case.

Our purpose is to investigate phase transition behavior when the order parameter space is described by the direct product between two groups. Then, hereafter, we focus

on the parameter region $J_3/J_1 < -1/4$ in the case of ferromagnetic J_1 . Throughout the paper, we use the interaction ratio $J_3/J_1 = -0.85355\cdots$ so that the ground state is represented by $k^* = \pi/2$ in Eq. (4). In this case, along one of three axes, the relative angle between nearest-neighbor spin pairs is 90-degree, while along the other axes, the relative angle is 45-degree in the ground-state spin configuration [see Fig. 2(b)]. When the period of lattice is set to 8, the commensurate spiral-spin configuration appears in the ground state. Then, in order to avoid the incompatible due to boundary effect, the linear dimension $L = 8n$ ($n \in \mathcal{N}$) is used and the periodic boundary conditions in all directions are imposed.

III. FINITE-TEMPERATURE PROPERTIES OF STACKED MODEL

In this section, we investigate finite-temperature properties of the Heisenberg model on a stacked triangular lattice with competing interactions given by Eq. (1) with $J_3/J_1 = -0.85355\cdots$ and $J_\perp/J_1 = 2$. Using Monte Carlo simulations with single-spin flip heat-bath method and the over-relaxation method,^{57,58} we calculate temperature dependence of physical quantities. Figures 3 (a) and 3 (b) show internal energy per site E and specific heat C for $L = 24, 32, 40$. The specific heat at the temperature T is given by

$$C = N \frac{\langle E^2 \rangle - \langle E \rangle^2}{T^2}, \quad (6)$$

where $\langle \mathcal{O} \rangle$ denotes the equilibrium value of the physical quantity \mathcal{O} . Here the Boltzmann constant is set to unity. As the lattice size increases, sudden change in the internal energy is observed at a temperature. In addition, the specific heat has a divergent single peak at the temperature. These behaviors indicate an existence of a finite-temperature phase transition. As will be shown in Sec. IV, the uniform magnetic susceptibility can be used as an indicator of the phase transition. To investigate the way of ordering, the temperature dependence of an order parameter is considered. The order parameter μ which can detect the C_3 symmetry breaking is defined by

$$\mu := \varepsilon_1 \mathbf{e}_1 + \varepsilon_2 \mathbf{e}_2 + \varepsilon_3 \mathbf{e}_3, \quad (7)$$

$$\varepsilon_\eta := \frac{1}{N} \sum_{\langle i,j \rangle_1 \parallel \text{axis } \eta} \mathbf{s}_i \cdot \mathbf{s}_j, \quad (8)$$

where the subscript η ($\eta = 1, 2, 3$) assigns the axis (see Fig. 1). The vectors \mathbf{e}_η are unit vectors along the axis η , i.e., $\mathbf{e}_1 = (1, 0)$, $\mathbf{e}_2 = (-1/2, \sqrt{3}/2)$, and $\mathbf{e}_3 = (-1/2, -\sqrt{3}/2)$. The temperature dependence of $\langle |\mu|^2 \rangle$ is shown in Fig. 3(c). The order parameter abruptly increases around the temperature at which the specific heat has a divergent peak. These results conclude that the phase transition is accompanied with the C_3 symmetry breaking.

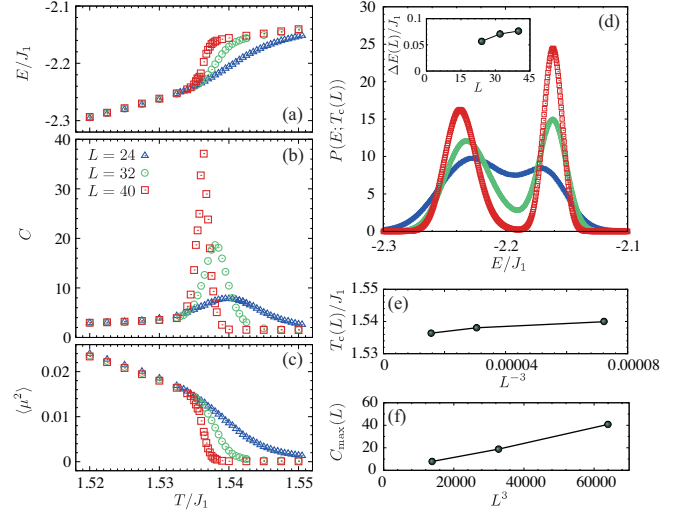


FIG. 3. (Color online) Temperature dependence of (a) internal energy per site E/J_1 , (b) specific heat C , and (c) order parameter $\langle |\mu|^2 \rangle$ which can detect the C_3 symmetry breaking of the model with $J_3/J_1 = -0.85355\cdots$ and $J_\perp/J_1 = 2$ for $L = 24, 32, 40$. (d) Probability distribution of the internal energy $P(E; T_c(L))$. Inset figure shows the lattice-size dependence of width between bimodal peaks $\Delta E(L)/J_1$. (e) $T_c(L)/J_1$ as a function of L^{-3} . (f) $C_{\max}(L)$ as a function of L^3 . Lines are just visual guides, and error bars in all figures are omitted for clarity since their sizes are smaller than the symbol size.

To decide the order of the phase transition, we calculate the probability distribution of internal energy at T , $P(E; T) = D(E) \exp(-NE/T)$, where $D(E)$ is density of states. When a system exhibits a first-order phase transition, the energy distribution $P(E; T)$ should be a bimodal structure at the temperature $T_c(L)$ for lattice size L . $T_c(L)$ is the temperature at which the specific heat becomes the maximum value $C_{\max}(L)$. To obtain $T_c(L)$ and $C_{\max}(L)$, we perform the reweighting method.⁵⁹ Figure 3(d) shows $P(E; T_c(L))$ for system sizes $L = 24, 32, 40$. As stated above, the bimodal structure in the energy distribution suggests a first-order phase transition.

To confirm whether the first-order phase transition behavior remains in the thermodynamic limit, we perform two types of analyses. The one is the finite-size scaling and the other is a naive analysis of probability distribution $P(E; T_c(L))$. The scaling relations for the first-order phase transition in d -dimensional systems⁶⁰ are given as

$$T_c(L) = aL^{-d} + T_c, \quad (9)$$

$$C_{\max}(L) \propto \frac{(\Delta E)^2 L^d}{4T_c^2}, \quad (10)$$

where T_c and ΔE are respectively the transition temperature and the latent heat in the thermodynamic limit. The coefficient of the first term in Eq. (9), a , is a constant. Figures 3 (e) and 3 (f) show the scaling plots

for $T_c(L)/J_1$ and $C_{\max}(L)$, respectively. Figure 3 (e) indicates T_c is a non-zero value in the thermodynamic limit. Figure 3 (f) shows almost linear dependence of $C_{\max}(L)$ as a function of L^3 . However, using the finite-size scaling, we cannot obtain the transition temperature and latent heat in the thermodynamic limit with high accuracy because of strong finite-size effect. Next, we directly calculate the size dependence of the width between bimodal peaks of energy distribution shown in Fig. 3 (d). The width for the lattice size L is represented by $\Delta E(L) = E_+(L) - E_-(L)$ where $E_+(L)$ and $E_-(L)$ are the average of the Gaussian in the high-temperature phase and that in the low-temperature phase, respectively. In the thermodynamic limit, each Gaussian becomes the delta-function and then, $\Delta E(L)$ converges to ΔE .⁶⁰ The inset of Fig. 3 (d) shows size dependence of the width $\Delta E(L)/J_1$. The width enlarges as the lattice size increases, which indicates the latent heat is non-zero value in the thermodynamic limit. The results shown in Fig. 3 conclude that the model given by Eq.(1) exhibits the first-order phase transition with the C_3 symmetry breaking at finite temperature.

We further investigate the way of spin ordering. As mentioned above, the order parameter space of the system is $SO(3) \times C_3$. It was confirmed that the C_3 symmetry breaks at the first-order phase transition point. In the antiferromagnetic Heisenberg model on a stacked triangular lattice with only nearest-neighbor interaction where the order parameter space is $SO(3)$, a single peak is observed in the temperature dependence of the specific heat.⁴¹ The peak indicates the finite-temperature phase transition between paramagnetic state and magnetic ordered state where the $SO(3)$ symmetry is broken. Then, in our model, the $SO(3)$ symmetry should break at the first-order phase transition point since the specific heat has a single peak corresponding to the first-order phase transition. To confirm the fact, we calculate the temperature dependence of the structure factor of spin:

$$S(\mathbf{k}) := \frac{1}{N} \sum_{i,j} \langle \mathbf{s}_i \cdot \mathbf{s}_j \rangle e^{-i\mathbf{k} \cdot (\mathbf{r}_i - \mathbf{r}_j)}, \quad (11)$$

which is the magnetic order parameter for spiral-spin states. When the magnetic ordered state described by \mathbf{k}^* where the $SO(3)$ symmetry is broken appears, $S(\mathbf{k}^*)$ becomes finite value in the thermodynamic limit. Figure 4 (a) shows the temperature dependence of the largest value of structure factors $S(\mathbf{k}^*)$ calculated by six wave vectors in Eq. (4). $S(\mathbf{k}^*)$ becomes zero in the thermodynamic limit above the first-order phase transition temperature. The structure factor $S(\mathbf{k}^*)$ becomes nonzero value at the first-order phase transition temperature. Moreover, as temperature decreases, the structure factor $S(\mathbf{k}^*)$ increases. The structure factors at $k_z = 0$ in the first Brillouin zone at several temperatures for $L = 40$ are also shown in Fig. 4 (b). As mentioned in Sec. II, spiral spin structure represented by \mathbf{k} is the same as that by $-\mathbf{k}$. Figure 4 (b) confirms that one distinct wave vector is chosen from three types of ordered vectors below

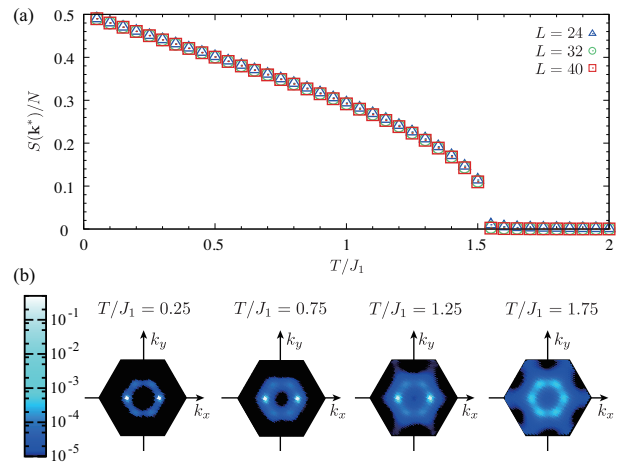


FIG. 4. (Color online) (a) Temperature dependence of the largest value of structure factors $S(\mathbf{k}^*)$ calculated by six wave vectors in Eq. (4) for $J_3/J_1 = -0.85355 \dots$ and $J_\perp/J_1 = 2$. Error bars are omitted for clarity since their sizes are smaller than the symbol size. (b) Structure factors at $k_z = 0$ in the first Brillouin zone at several temperatures for $L = 40$.

the first-order phase transition point, which is another evidence of the C_3 symmetry breaking at the first-order phase transition temperature.

Before we end this section, let us mention a phase transition nature in the J_1 - J_2 Heisenberg model with interlayer interaction J_\perp on a stacked triangular lattice. In Refs. 50–53, the authors studied phase transition behavior of the model when J_1 and J_2 are antiferromagnetic interactions. For large J_2/J_1 , a phase transition between paramagnetic phase and ordered incommensurate spiral-spin structure occurs at finite temperature. In this case, the order parameter space is $SO(3) \times C_3$ and a second-order phase transition occurs,⁵⁰ which differs from the obtained result in this section. However, in frustrated spin systems, different phase transition nature happens even when the order parameter space is the same as other models. For example, in the J_1 - J_3 Heisenberg model on a triangular lattice, a first-order phase transition with the three-fold symmetry breaking occurs when $J_3/J_1 < -1/4$ and $J_1 > 0$. It is well-known that the simplest model which exhibits a phase transition with the three-fold symmetry breaking is the three-state ferromagnetic Potts model.⁶¹ The three-state ferromagnetic Potts model in two-dimension exhibits a second-order phase transition. Then, it is no wonder that our obtained result differs from the results in previous study.⁵⁰

IV. DEPENDENCE OF INTERLAYER INTERACTION

In this section, we study interlayer-interaction dependence of phase transition behavior. Here we fix the interaction ratio $J_3/J_1 = -0.85355 \dots$ at which the ground

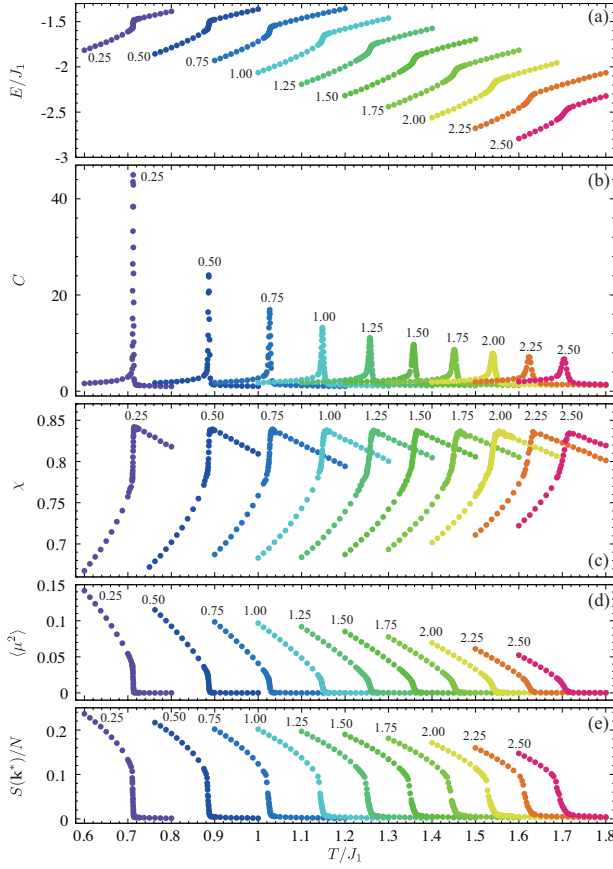


FIG. 5. (Color online) Interlayer interaction J_{\perp}/J_1 dependence of (a) internal energy per site E/J_1 , (b) specific heat C , (c) uniform magnetic susceptibility χ , (d) order parameter $\langle |\mu|^2 \rangle$ which can detect the C_3 symmetry breaking, and (e) the largest value of structure factors $S(\mathbf{k}^*)$ calculated by six wave vectors in Eq. (4) for $L = 24$. Error bars in all figures are omitted for clarity since their sizes are smaller than the symbol size.

state is represented by $k^* = \pi/2$ in Eq. (4) as in the previous section. In the previous section, we considered the case that $J_{\perp}/J_1 = 2$. We found that the first-order phase transition with the C_3 symmetry breaking occurs, and breaking of the $SO(3)$ symmetry at the first-order phase transition point was confirmed.

Figure 5 shows the temperature dependence of physical quantities for $L = 24$ with several interlayer interactions $0.25 \leq J_{\perp}/J_1 \leq 2.5$ fixing $J_3/J_1 = -0.85355\dots$. Figure 5 (a) shows the internal energy as a function of temperature, which displays that the temperature at which the sudden change of the internal energy appears increases as J_{\perp}/J_1 increases. In other words, Fig. 5 (a) indicates that the first-order phase transition temperature monotonically increases as a function of J_{\perp}/J_1 . In addition, the energy difference between high-temperature phase and low-temperature phase decreases as J_{\perp}/J_1 increases. These behaviors are supported by the temperature dependence of the specific heat shown in Fig. 5

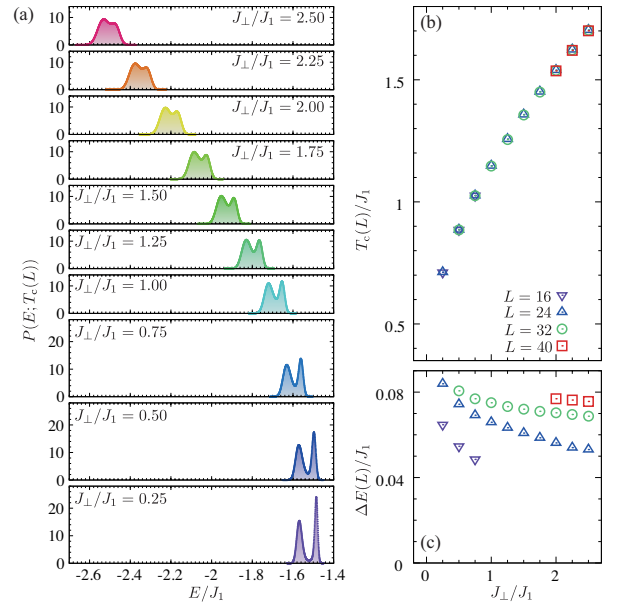


FIG. 6. (Color online) (a) Interlayer interaction J_{\perp}/J_1 dependence of the probability distribution of internal energy $P(E; T_c(L))$ when the specific heat becomes the maximum value for $L = 24$. (b) J_{\perp}/J_1 -dependence of $T_c(L)/J_1$ at which the specific heat becomes the maximum value for $L = 16 - 40$. (c) J_{\perp}/J_1 -dependence of width between bimodal peaks of the energy distribution $\Delta E(L)/J_1$. Error bars in all figures are omitted for clarity since their sizes are smaller than the symbol size.

(b). Furthermore, in the specific heat, no peaks except the first-order phase transition temperature are observed by changing the value of J_{\perp}/J_1 . Figure 5 (c) shows the uniform magnetic susceptibility χ which is calculated by

$$\chi = \frac{NJ_1 \langle |\mathbf{m}|^2 \rangle}{T}, \quad \mathbf{m} = \frac{1}{N} \sum_i \mathbf{s}_i, \quad (12)$$

where \mathbf{m} is the uniform magnetization. The uniform magnetic susceptibility has the sudden change at the first-order phase transition temperature. As stated in Sec. III, it can be used as an indicator of the first-order phase transition. Note that the magnetic susceptibility of the model with J_{\perp} differs from that with $-J_{\perp}$. However, the sudden change in χ at the first-order phase transition temperature is also observed when the interlayer interaction is antiferromagnetic. We obtain the Curie-Weiss temperature from the magnetic susceptibility for several J_{\perp}/J_1 's including the case of antiferromagnetic J_{\perp} , which will be shown in Appendix A. In addition, Figs. 5 (d) and 5 (e) confirm that phase transitions always accompany the C_3 lattice rotational symmetry breaking and breaking of the global rotational symmetry of spin, the $SO(3)$ symmetry, for the considered J_{\perp}/J_1 's, respectively.

Next, in order to consider J_{\perp}/J_1 -dependence of latent heat, we calculate probability distribution of internal en-

ergy $P(E; T_c(L))$ for several values of J_\perp/J_1 shown in Fig. 6 (a). The width between bimodal peaks decreases as J_\perp/J_1 increases. Furthermore, we calculate interlayer-interaction dependences of $T_c(L)/J_1$ and $\Delta E(L)/J_1$ for $L = 16 - 40$ which are shown in Figs. 6 (b) and 6 (c). As J_\perp/J_1 increases, $T_c(L)/J_1$ monotonically increases and $\Delta E(L)/J_1$ decreases for each lattice size. In addition, $\Delta E(L)/J_1$ increases as the system size increases. $\Delta E(L)/J_1$ in the thermodynamic limit corresponds to the latent heat. Thus, Fig. 6 (c) suggests that the latent heat decreases as J_\perp/J_1 increases in the thermodynamic limit.

V. DISCUSSION AND CONCLUSION

In this paper, nature of phase transition of the Heisenberg model on a stacked triangular lattice was studied by Monte Carlo simulations. In our model, there are three kinds of interactions: ferromagnetic nearest-neighbor interaction J_1 and antiferromagnetic third nearest-neighbor interaction J_3 in each triangular layer, and ferromagnetic nearest-neighbor interlayer interaction J_\perp . When $J_3/J_1 < -1/4$, the ground state is a spiral-spin structure in which the C_3 symmetry is broken as in the case of two-dimensional J_1 - J_3 Heisenberg model on a triangular lattice.^{32,33} Then the order parameter space in the case is described by $SO(3) \times C_3$.

In Sec. III, we studied finite-temperature properties of the system with $J_3/J_1 = -0.85355 \dots$ and $J_\perp/J_1 = 2$. We found that a first-order phase transition takes place at finite temperature. The temperature dependence of the order parameter indicates that the C_3 symmetry breaks at the transition temperature, which is the same feature as two-dimensional case.^{32,33} We also calculated the temperature dependence of the structure factor at the wave vector representing the ground state, which is the magnetic order parameter for spiral-spin states. The result shows that the $SO(3)$ symmetry breaks at the transition temperature.

In Sec. IV, we investigated the interlayer interaction effect for nature of phase transitions. We confirmed that the first-order phase transition occurs for $0.25 \leq J_\perp/J_1 \leq 2.5$ and $J_3/J_1 = -0.85355 \dots$ which was used in Sec. III. We could not determine the existence of the first-order phase transition for $J_\perp/J_1 < 0.25$ or $J_\perp/J_1 > 2.5$. In the parameter ranges, the width of two peaks in the probability distribution of the internal energy cannot be estimated easily because of the finite-size effect. It is a remaining problem to determine whether a second-order phase transition which was observed in the J_1 - J_2 Heisenberg model on a stacked triangular lattice when the order parameter space is $SO(3) \times C_3$ ⁵⁰ occurs for large J_\perp/J_1 . As the ratio J_\perp/J_1 increases, the first-order phase transition temperature monotonically increases but the latent heat decreases. The fact is opposite to the behavior observed in unfrustrated systems in which a phase transition occurs with discrete symmetry breaking. For

example, the q -state Potts model with ferromagnetic intralayer and interlayer interactions ($q \geq 3$) is a fundamental model which exhibits a temperature-induced first-order phase transition with q -fold symmetry breaking.⁶¹ From a mean-field analysis of the ferromagnetic Potts model, as the interlayer interaction increases, both the transition temperature and the latent heat increase. In conventional systems, both the transition temperature and the latent heat are expressed by the value of an effective interaction obtained by a characteristic temperature such as the Curie-Weiss temperature. However, in our model, the Curie-Weiss temperature does not characterize the first-order phase transition as will be shown in Appendix A. Then our obtained result is an unusual behavior. To investigate the essence of the obtained results is a remaining problem.

ACKNOWLEDGMENT

R.T. is partially supported by Grand-in-Aid for Scientific Research (C) (25420698) and National Institute for Materials Science (NIMS). S.T. is partially supported by Grand-in-Aid for JSPS Fellows (23-7601). The computations in the present work were performed on computers at the Supercomputer Center, Institute for Solid State Physics, University of Tokyo.

Appendix A: Interlayer-interaction dependence of the Curie-Weiss Temperature

In this section, we obtain the Curie-Weiss temperature for several J_\perp/J_1 's including the case of antiferromagnetic interlayer interaction. Here we also use the interaction ratio $J_3/J_1 = -0.85355 \dots$ which is used in Secs. III and IV. As mentioned in Sec. II, phase transition behavior of the model with J_\perp is the same as that with $-J_\perp$, which is proved by the local gauge transformation. However, the Curie-Weiss temperature for J_\perp differs from that for $-J_\perp$. Figure 7 (a) shows the inverse of the magnetic susceptibility χ^{-1} as a function of temperature in high-temperature region for $L = 24$. In general, the temperature dependence of the magnetic susceptibility at high temperatures is expressed as

$$\chi = \frac{A}{T - \theta_{CW}}, \quad (A1)$$

where A is the Curie constant and θ_{CW} is the Curie-Weiss temperature. The Curie-Weiss temperature θ_{CW} represents a characteristic temperature of magnetic systems. The interlayer-interaction dependence of the Curie-Weiss temperature is shown in Fig. 7 (b). The Curie-Weiss temperature dependence is not symmetric about the origin. The first-order phase transition temperature of the system with J_\perp is the same as that with $-J_\perp$. Then the transition temperature does not relate to the Curie-Weiss temperature.

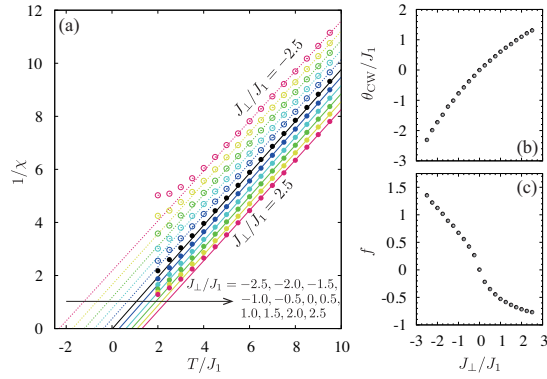


FIG. 7. (Color online) (a) Inverse of the magnetic susceptibility χ^{-1} as a function of temperature with $J_3/J_1 = -0.85355 \dots$ and several J_\perp/J_1 's for $L = 24$. The lines are obtained by the least-squares estimation. (b) J_\perp/J_1 -dependence of the Curie-Weiss temperature. (c) J_\perp/J_1 -dependence of the ratio $f = -\theta_{CW}/T_c$.

Next we consider J_\perp/J_1 -dependence of the ratio of two characteristic temperatures $f := -\theta_{CW}/T_c$. In frustrated systems, f is a useful quantity to express “degree of frustration” and is called as frustration parameter. Figure 7 (c) depicts the interlayer-interaction dependence of f . The value of f is not a characteristic quantity which expresses the nature of first-order phase transition as well as the Curie-Weiss temperature.

-
- * tamura.ryo@nims.go.jp
† shu-t@chem.s.u-tokyo.ac.jp
- ¹ G. Toulouse, Commun. Phys. (London) **2**, 115 (1977).
 - ² R. Liebmann, *Statistical Mechanics of Periodic Frustrated Ising Systems* (Springer-Verlag, Berlin/Heidelberg GmbH, Heidelberg, 1986).
 - ³ H. Kawamura, J. Phys.: Condens. Matter **10**, 4707 (1998).
 - ⁴ *Frustrated Spin Systems*, edited by H. T. Diep (World Scientific, Singapore, 2005).
 - ⁵ B. W. Southern, La Physique au Canada, **68**, 83 (2012).
 - ⁶ J. Villain, R. Bidaux, J. -P. Carton, and R. Conte, J. Phys. (Paris) **41**, 1263 (1980).
 - ⁷ C. L. Henley, Phys. Rev. Lett. **62**, 2056 (1989).
 - ⁸ Y. Shimizu, K. Miyagawa, K. Kanoda, M. Maesato, and G. Saito, Phys. Rev. Lett. **91**, 107001 (2003).
 - ⁹ S. Nakatsuji, Y. Nambu, H. Tonomura, O. Sakai, S. Jonas, C. Broholm, H. Tsunetsugu, Y. Qiu, Y. Maeno, Science (London) **309**, 1697 (2005).
 - ¹⁰ S. Tanaka and S. Miyashita, J. Phys. Soc. Jpn. **76**, 103001 (2007).
 - ¹¹ L. Balents, Nature **464**, 199 (2010).
 - ¹² R. Ishii, S. Tanaka, K. Onuma, Y. Nambu, M. Tokunaga, T. Sakakibara, N. Kawashima, Y. Maeno, C. Broholm, D. P. Gautreaux, J. Y. Chan, and S. Nakatsuji, Europhys. Lett. **94**, 17001 (2011).
 - ¹³ H. Katsura, N. Nagaosa, and A. V. Balatsky, Phys. Rev. Lett. **95**, 057205 (2005).
 - ¹⁴ T. Kimura, J. C. Lashley, and A. P. Ramirez, Phys. Rev. B **73**, 220401(R) (2006).
 - ¹⁵ S. W. Cheong and M. Mostovoy, Nat. Mater. **6**, 13 (2007).
 - ¹⁶ Y. Tokura and S. Seki, Adv. Mater. **22**, 1554 (2010).
 - ¹⁷ T. Arima, J. Phys. Soc. Jpn. **80**, 052001 (2011).
 - ¹⁸ N. Nagaosa, J. Sinova, S. Onoda, A. H. MacDonald, and N. P. Ong, Rev. Mod. Phys. **82**, 1539 (2010).
 - ¹⁹ S. Tanaka, H. Katsura, and N. Nagaosa, Phys. Rev. Lett. **97**, 116404 (2006).
 - ²⁰ S. Miyashita and H. Shiba, J. Phys. Soc. Jpn. **53**, 1145 (1984).
 - ²¹ H. Kawamura and S. Miyashita, J. Phys. Soc. Jpn. **53**, 4138 (1984).
 - ²² D. Loison, Chapter 4 in *Frustrated Spin Systems*, edited by H. T. Diep (World Scientific, Singapore, 2005).
 - ²³ T. Okubo, S. Chung, and H. Kawamura, Phys. Rev. Lett. **108**, 017206 (2012).
 - ²⁴ R. Tamura, S. Tanaka, and N. Kawashima, Phys. Rev. B **87**, 214401 (2013).
 - ²⁵ N. D. Mermin and H. Wagner, Phys. Rev. Lett. **17**, 1133 (1966).
 - ²⁶ H. Kawamura, A. Yamamoto, and T. Okubo, J. Phys. Soc. Jpn. **79**, 023701 (2010).
 - ²⁷ H. Kawamura, J. Phys.: Conf. Ser. **320**, 012002 (2011).
 - ²⁸ J. -C. Dornge, C. Lhuillier, L. Messio, L. Pierre, and P. Viot, Phys. Rev. B, **77**, 172413 (2008).
 - ²⁹ Y. Ajiro, H. Kikuchi, S. Sugiyama, T. Nakashima, S. Shamoto, N. Nakayama, M. Kiyama, N. Yamamoto, and Y. Oka, J. Phys. Soc. Jpn. **57**, 2268 (1988).
 - ³⁰ H. Yamaguchi, S. Kimura, M. Hagiwara, Y. Nambu, S. Nakatsuji, Y. Maeno, and K. Kindo, Phys. Rev. B **78**, 180404(R) (2008).
 - ³¹ M. Hemmida, H. -A. Krug von Nidda, and A. Loidl, J. Phys. Soc. Jpn. **80**, 053707 (2011).
 - ³² R. Tamura and N. Kawashima, J. Phys. Soc. Jpn. **77**, 103002 (2008).
 - ³³ R. Tamura and N. Kawashima, J. Phys. Soc. Jpn. **80**, 074008 (2011).
 - ³⁴ D. Loison and P. Simon, Phys. Rev. B **61**, 6114 (2000).
 - ³⁵ C. Weber, L. Capriotti, G. Misguich, F. Becca, M. Elhajal, and F. Mila, Phys. Rev. Lett. **91**, 177202 (2003).
 - ³⁶ E. M. Stoudenmire, S. Trebst, and L. Balents, Phys. Rev. B **79**, 214436 (2009).
 - ³⁷ S. Okumura, H. Kawamura, T. Okubo, and Y. Motome, J. Phys. Soc. Jpn. **79**, 114705 (2010).
 - ³⁸ R. Tamura, S. Tanaka, and N. Kawashima, Prog. Theor. Phys. **124**, 381 (2010).
 - ³⁹ S. Tanaka, R. Tamura, and N. Kawashima, J. Phys.: Conf. Ser. **297**, 012022 (2011).

- ⁴⁰ S. Tanaka and R. Tamura, J. Phys.: Conf. Ser. **320**, 012025 (2011).
- ⁴¹ H. Kawamura, J. Phys. Soc. Jpn. **54**, 3220 (1985).
- ⁴² H. Kawamura, J. Phys. Soc. Jpn. **61**, 1299 (1992).
- ⁴³ A. Pelissetto, P. Rossi, and E. Vicari, Phys. Rev. B **65**, 020403(R) (2002).
- ⁴⁴ P. Calabrese, P. Parruccini, A. Pelissetto, and E. Vicari, Phys. Rev. B **70**, 174439 (2004).
- ⁴⁵ A. K. Murtazaev and M. K. Ramazanov, Phys. Rev. B **76**, 174421 (2007).
- ⁴⁶ G. Zumbach, Phys. Rev. Lett. **71**, 2421 (1993).
- ⁴⁷ M. Tissier, B. Delamotte, and D. Mouhanna, Phys. Rev. Lett. **84**, 5208 (2000).
- ⁴⁸ M. Zelli, K. Boese, and B. W. Southern, Phys. Rev. B **76**, 224407 (2007).
- ⁴⁹ V. Thanh Ngo and H. T. Diep, Phys. Rev. E **78**, 031119 (2008).
- ⁵⁰ D. Loison and H. T. Diep, Phys. Rev. B **50**, 16453 (1994).
- ⁵¹ A. K. Murtazaev, M. K. Ramazanov, and M. K. Badiev, Bulletin of the Russian Academy of Science, Physics **74**, 1042 (2010).
- ⁵² A. K. Murtazaev, M. K. Ramazanov, and M. K. Badiev, Bulletin of the Russian Academy of Science, Physics **75**, 1042 (2011).
- ⁵³ M. K. Ramazanov, JETP Letters **94**, 311 (2011).
- ⁵⁴ A. Yoshimori, J. Phys. Soc. Jpn. **14**, 807 (1959).
- ⁵⁵ T. Nagamiya, *Solid State Physics Vol. 20* (Academic Press Inc., New York, 1967).
- ⁵⁶ Th. Jolicœur, E. Dagotto, E. Gagliano, and S. Bacci, Phys. Rev. B **42**, 4800 (1990).
- ⁵⁷ M. Creutz, Phys. Rev. D **36**, 515 (1987).
- ⁵⁸ K. Kanki, D. Loison, and K. D. Schotte, Eur. Phys. J. B **44**, 309 (2005).
- ⁵⁹ A. M. Ferrenberg and R. H. Swendsen, Phys. Rev. Lett. **61** 2635 (1988).
- ⁶⁰ M. S. S. Challa, D. P. Landau, and K. Binder, Phys. Rev. B **34**, 1841 (1986).
- ⁶¹ F. Y. Wu, Rev. Mod. Phys. **54**, 235 (1982).